Protein Partitioning in Two-Phase Aqueous Polymer Systems. 2. On the Free Energy of Mixing Globular Colloids and Flexible Polymers

Nicholas L. Abbott,† Daniel Blankschtein,* and T. Alan Hatton

Department of Chemical Engineering, Massachusetts Institute of Technology, Cambridge, Massachusetts 02139

Received December 27, 1991; Revised Manuscript Received March 31, 1992

ABSTRACT: The free energy of mixing globular colloids (spheroidal and ellipsoidal) and singly-dispersed flexible and linear polymer chains in an incompressible solvent (continuum) is formulated. The deformable and penetrable nature of the polymer coils (apparent in both polymer–polymer and polymer–colloid interactions), as well as the rigid and impenetrable nature of the globular colloids, is incorporated in evaluating the contributions of repulsive steric and short-ranged attractive interactions to the free energy of mixing. The interaction potentials, evaluated by combining a Monte Carlo scheme and the polymer solution theories of Flory and Flory and Krigbaum, are cast in terms of effective hard-sphere potentials (which are nonadditive) in order to evaluate the osmotic pressure and subsequently derive the chemical potentials of the colloid and the polymer at constant temperature and pressure. With an increase in polymer molecular weight, the increased deformability and penetrability of the polymer coils to the colloid can lead to *qualitatively* different trends in the molecular weight dependence of the chemical potential of the colloid, as compared to the case where the polymer coil is treated as a rigid body characterized by its radius of gyration. The influence of a weak and short-ranged attraction between the polymer-coil segments and the colloids on the predicted thermodynamic properties also reflects the increasing diffuseness of the polymer coils with increasing polymer molecular weight. This theoretical framework is used to predict the partitioning behavior of globular proteins in a two-phase aqueous poly(ethylene oxide) (PEO)–dextran system. To predict experimentally observed trends in protein partitioning behavior with increasing PEO molecular weight, the inclusion of both repulsive steric and weak attractive interactions is necessary. The strength of the attractive interaction between a polymer-coil segment and the protein molecule appears to increase with protein size up to approximately 0.1 kT, although the overall interaction (which includes the steric interaction) remains repulsive. The effect of shape asymmetry on the predicted partitioning behavior of an ellipsoidal bovine serum albumin protein molecule is evaluated and found to be different from that corresponding to a spherical protein having the same volume. This observation suggests that protein shape (conformation) can be a significant factor in determining the partitioning of proteins in two-phase aqueous polymer systems.

1. Introduction

An important contribution to the free energy of mixing of solutions which contain colloids and flexible polymers arises from the translational and configurational degrees of freedom available to these macromolecular species.[1-3] Specifically, the translational degrees of freedom arise from the many positions that the centers of mass of the species can assume, while the configurational degrees of freedom reflect the different conformations that the flexible macromolecules can adopt for a fixed position of their centers of mass. In all macromolecular systems, the existence of a variety of interactions, for example, weak attractive interactions of the van der Waals type or strong repulsive steric (excluded-volume) interactions, restricts the translations and the configurations which can be sampled by the species within the system. While the translations are influenced by the interactions between macromolecules, the nature of these interactions can, in general, also reflect their internal configurational states. It follows, therefore, that the configurations of macromolecules can also reflect, in general, a balance of the interactions *within* and *between* species. However, when there are strong cohesive interactions within macromolecules (and particles) and only weak interactions between species, their configurational states (the shapes) are only weakly perturbed by interparticle interactions. An example of a system where there *is* a clear separation of the intraparticle and interparticle interactions is a solution of gold or silica sols where the individual sols are held together by short-ranged, yet very strong, "chemical" forces (metallic or covalent bonds, respectively), and only weak van der Waals interactions exist between the sols.[4,5] In contrast, many other colloidal systems exhibit rather weak interactions within the colloidal particles. In that case, the configurational state of the colloidal particles is greatly influenced by both the interactions within the particles and between particles. An example of such a system is a micellar solution containing aggregates of surfactant molecules (micelles).[6-8] In this case, the "physical" forces, such as hydrophobic forces, which in aqueous solution are responsible, in part, for the self-assembly of the surfactant molecules into fluidlike and deformable aggregates, are similar in nature and strength to the interactions occurring between micellar aggregates. Indeed, the wide variety of shapes and sizes of micelles that are observed experimentally in aqueous surfactant solutions reflects, in general, the delicate nature of the balance between intramicellar and intermicellar interactions.

Another class of systems in which the above-mentioned considerations are important is aqueous solutions containing globular proteins and flexible linear polymers.[9-11] Changes in the configurational state of flexible linear polymers in response to variations in solution conditions, such as polymer concentration, have been documented both experimentally and theoretically.[3,12-14] The average radius of gyration of a polymer coil within an entangled polymer network, for example, decreases with increasing polymer concentration.[12-14] Indeed, under certain con-

* To whom correspondence should be addressed.
† Present address: Department of Chemistry, Harvard University, Cambridge, MA 02138.

0024-9297/92/2225-3917$03.00/0

ditions, a concentration-dependent collapse of the chain to a globular state is observed.[15] Similarly, proteins are delicately folded linear polypeptide chains having average conformations which generally reflect a balance between the "physical" and "chemical" forces acting within the polypeptide chain, as well as the interactions occurring between the polypeptide chain and its surrounding environment.[16] For example, upon addition of anionic surfactant molecules, such as sodium dodecyl sulfate, or other denaturants, such as urea, to an aqueous protein solution, a protein will typically undergo a gross conformational change from a highly structured and compact globular state to a more expanded and tenuous random-coil conformation.[17,18]

In a recent paper,[19] hereafter referred to as paper 1, the important role of the interactions between polymers and proteins in determining the protein partitioning behavior in phase-separated aqueous polymer systems was emphasized. In particular, the influence of these interactions on the free energy of mixing proteins and polymers was examined in the context of a scaling-thermodynamic formulation. In the course of that work many of the more general issues associated with the evaluation of the free energy of mixing macromolecules were encountered. Specifically, the need to consider the potential coupling of interactions *between* macromolecules and interactions *within* macromolecules was discussed. The purpose of the present paper is twofold: (i) to address many of the important and unresolved issues related to the free energy of mixing globular proteins and flexible linear polymers in aqueous solution which were identified in paper 1 and (ii) to shed light on the more general problem of the role of deformability and penetrability in evaluating the free energy of colloidal systems, where the deformability of the particles arises from the coupling of intracolloid and intercolloid interactions.

For the sake of brevity, the reader is referred to two recent reviews of previous theoretical work dealing with protein partitioning in two-phase aqueous polymer systems.[20,21] Below we summarize only the essential points needed for the theoretical developments presented in this paper.

As was discussed in paper 1, in the poly(ethylene oxide) (PEO)–dextran–water two-phase system, a transition occurs in the nature of the top PEO-rich phase, from a solution of identifiable polymer coils to a solution of extensively interpenetrating polymers, with increasing PEO molecular weight.[19] In this transition region, the protein partition coefficient, defined as the ratio of the protein concentrations in the top and bottom phases, respectively, was observed to decrease.[22,23] However, for sufficiently high molecular weights of PEO, where PEO was extensively entangled, the protein partition coefficient was observed to be independent of the PEO molecular weight, reflecting the fact that the protein "lost sight" of the PEO coils within the entangled polymer mesh.[19] Furthermore, it was observed that the ability of a protein to "sense" the transition in the underlying solution structure correlated with the size of the protein species. Specifically, large proteins, for example, catalase (R_p = 51 Å), exhibited large changes in their partition coefficients, whereas small proteins, such as cytochrome *c* (R_p = 17 Å), were insensitive to changes in the structure of the solution.[19] For the purpose of the present paper we will confine our treatment to polymer solutions in the "dilute" regime, since it is in this regime that one observes the greatest sensitivity of the protein partition coefficient to changes in PEO molecular weight.[19] In a separate paper, we will discuss the rather different situation of proteins interacting with entangled polymer solutions.[24]

In a typical PEO-rich solution phase which contains low molecular weight PEO ($M < 10\,000$ Da), the individual polymer coils which interact with the protein may be larger or smaller than the protein molecules.[19] It is important to point out that this situation is in sharp contrast with the extensively-studied case where a colloid, for example, a silica sol, interacts *sterically* with a flexible polymer that is significantly smaller than the sol.[25-30] In that case, the polymer coil and sol are essentially impenetrable to each other, so that, in effect, one can represent the steric interaction potential between the two particles as a simple hard-sphere repulsion.[25-30] Note that the range of this steric repulsion is given by the sum of the globular colloid radius and the polymer radius of gyration, R_g.[25-30] In contrast, in the protein partitioning case, where the polymer-coil size can become large compared to the size of the globular protein, the polymer coil can no longer be represented effectively as an impenetrable sphere of size R_g since an increased number of polymer-coil configurations allow the protein to penetrate the volume occupied, on average, by the polymer.[19] To model this interesting situation and at the same time be able to exploit some of the available useful results for hard-sphere systems, we have chosen to generalize the conventional treatment of excluded-volume hard-sphere interactions. Specifically, we have represented the polymer coil as an effective hard-sphere whose size reflects the permeability of the polymer coil toward the protein. In other words, due to the penetrable and diffuse nature of the polymers, one expects that, as the polymer molecular weight increases, the *effective hard-sphere size* associated with the polymer should increase more slowly than that corresponding to a rigid impermeable particle. It is this new physical situation, dealing with excluded-volume interactions between particles possessing different degrees of penetrability, which does not appear to have received much attention in the past, but which is essential to the treatment of protein partitioning in two-phase aqueous polymer systems, that we address in this paper. Indeed, in section 6 we show that if the penetrability of the polymer coil to the protein is neglected, within the context of our theoretical framework, *qualitatively* different trends in the molecular-weight dependence of the protein partition coefficient are predicted.

In paper 1 of this series it was shown that, under certain experimental conditions (see section 2),[19] the change in the logarithm of the protein partition coefficient, $\Delta \ln K_p$, accompanying a change in PEO molecular weight can be related simply to the change in the standard-state chemical potential of the protein, $\Delta\mu^\circ_{p,t}$, in the top (t) PEO-rich polymer solution phase, that is

$$\Delta \ln K_p = -\frac{\Delta\mu^\circ_{p,t}}{kT} \tag{1}$$

where k is the Boltzmann constant and T is the absolute temperature. The standard-state chemical potential of the protein in the top phase corresponds to the free-energy change upon introducing a single protein molecule into the top polymer solution phase from a phase containing pure solvent. Therefore, this term captures the effects of the direct interactions of the protein with the polymers as well as the influence of polymer–polymer interactions on the protein. Note that protein–protein interactions are not considered because in the limit of vanishing protein concentration, corresponding to the experimental conditions,[22,23] they make a negligible contribution to the observed partitioning behavior. In paper 1, mathemat-

ically-simple geometric and scaling arguments were developed to probe the *qualitative* form of the standard-state protein chemical potential, and thus the protein partition coefficient, reflecting both protein-polymer and polymer–polymer interactions.[19] A picture emerged which suggested that the change in the partition coefficients of proteins, which is observed to accompany a change in the PEO molecular weight, M_2, reflects a delicate balance of several competing factors. First, the influence of steric interactions between proteins and polymers on $\Delta \ln K_p$ is to increase the protein partition coefficient with an increase in M_2, a behavior which is *opposite* to that observed experimentally. Second, the influence of the polymer–polymer interactions is to decrease $\Delta \ln K_p$ with increasing M_2, a behavior which is consistent with that observed experimentally.[19] However, within the framework of the scaling-thermodynamic approach presented in paper 1, due to (i) the truncation of certain expansions at second order in the expansion parameter, $(N_2/V)U_2$, where N_2/V is the number density of polymer coils in the solution and U_2 is the polymer–polymer effective excluded volume, (ii) the unknown *precise* values of the polymer–polymer excluded volume, U_2, and (iii) the additional influence of polymer–polymer excluded-volume effects (within a polymer coil) on the magnitude of the protein–polymer excluded volume, U_p, it became evident that, in order to evaluate the relative roles of the protein–polymer and polymer–polymer interactions on the predicted protein partitioning behavior, a more quantitative approach was required.

In view of the possibility that steric effects alone could not predict the observed protein partitioning behavior, in paper 1 we also examined the influence of a weak attractive interaction between the protein molecules and the PEO coils on the standard-state chemical potential of the protein. For the sake of brevity the reader is referred to paper 1 where a detailed discussion of this term is presented and the possible physical origins of the attraction are discussed. However, it is pertinent to mention that while the attractive interaction between a PEO coil and a protein molecule was shown to increase with increasing PEO molecular weight, when the opposing influence of the decreasing number density of polymer coils, N_2/V, was included, an increase in the standard-state protein chemical potential, and hence a decrease in the protein partition coefficient, was predicted. Recall that this trend in the protein partition coefficient is consistent with that observed experimentally.[22,23] However, we could not estimate the strength of the attraction needed to account for the observed partitioning behavior, as this required evaluating the *additive* effects of steric and attractive interactions on the protein chemical potential. Such a *quantitative* prediction was beyond the scope of paper 1, where the aim was to establish a sound physical description of these systems as a basis for more detailed theoretical formulations. In this spirit, using paper 1 as the foundation, we present here a more quantitative account of protein partitioning in two-phase aqueous polymer systems.

Each of the issues outlined above is addressed in this paper, and, in particular, we develop a quantitative account of protein–polymer and polymer–polymer interactions, including the relative importance of their contributions to the standard-state protein chemical potential. We reveal that very weak attractive interactions can have a marked effect on the *qualitative nature* of the predicted protein partitioning behavior. In these evaluations, by combining liquid-state[31-33] and dilute polymer-solution theories,[34-36] along with a simple Monte Carlo evaluation,[37-39] we include (1) the influence of the deformability and permeability of the polymer coils on their interactions with globular proteins, (2) the partial permeability of polymer coils to each other (which varies with the solvent quality), and (3) the contributions of higher-order interactions between polymer coils and proteins. In addition, we investigate the influence of the protein shape on the partitioning behavior of proteins. Specifically, we evaluate the influence of deviations from sphericity (ellipsoidal shape) on the predicted standard-state protein chemical potential.

The remainder of the paper is organized as follows. In section 2, a general thermodynamic framework that relates thermodynamic quantities at constant solvent chemical potential to those at constant pressure is developed. Within this framework, using an equation of state for a binary hard-sphere mixture, the chemical potentials of the hard spheres are evaluated. In section 3, the components of the hard-sphere mixture are identified with the protien and the polymers, and the effective hard-sphere interaction potentials describing steric protein–polymer and polymer–polymer interactions are evaluated. Subsequently, in section 4, within the thermodynamic framework at constant pressure, the protein chemical potential in solutions containing flexible linear polymer molecules is evaluated. The dependence of the standard-state protein chemical potential on polymer molecular weight as well as on protein shape and size is also reported. In section 5, the additional effect of weak attractive protein–polymer interactions on the protein chemical potential is evaluated. In section 6, we discuss our findings and compare our predictions with earlier thermodynamic formulations of protein partitioning in two-phase aqueous polymer systems.

2. Thermodynamic Framework

As discussed in paper 1, under the experimentally accessible conditions of (i) vanishing protein concentration, (ii) essentially constant weight fractions of polymers in the coexisting phases, (iii) negligible dextran concentration in the PEO-rich phase, and (iv) negligible PEO concentration in the dextran-rich phase, the change in the protein partition coefficient with PEO molecular weight can be related simply to the standard-state chemical potential of the protein (see eq 1).[19] Note that for the range of conditions over which we compare our theoretical formulation with experiments, electrostatic interactions, due to the charged nature of the proteins and salts, do not determine the observed protein partitioning behavior. Therefore, we have not included electrostatic interactions in this theoretical formulation. In general, however, a theoretical description of protein partitioning which is applicable to all experimental conditions will require the incorporation of electrostatic effects. Since the system pressure is held constant in the experimental measurement of the protein partition coefficients, we present here an evaluation of the chemical potentials of the protein and PEO in an ensemble at constant pressure. For the evaluation of the thermodynamic properties of solutions containing solvent, salts, polymers, and proteins we treat the species as incompressible and approximate the solvent in the presence of salts as a structureless continuum, which is justified by the large size of the proteins and polymers as compared to that of the solvent molecules. The present treatment contrasts with that presented in paper 1, where a simplifying approximation was made and the protein chemical potential was evaluated holding constant the solvent chemical potential.[19] A comparison of the pre-

dicted standard-state protein chemical potential at constant pressure, P, with that at constant solvent chemical potential, μ_1, is presented and further discussed in section 6.

In Appendix A, a derivation is given of a general thermodynamic framework relating the chemical potential of species i in an incompressible solvent at constant pressure to that at constant solvent chemical potential. This development is particularly useful because it enables us to make use of some existing analytical results for the chemical potentials of hard-sphere mixtures which were derived at constant solvent chemical potential.[40] It is noteworthy that in the protein partitioning case the evaluation of the protein and polymer chemical potentials is simplified considerably by the fact that we are concerned with the limit of vanishing protein concentration, namely, $\phi_p \to 0$.[19] In this limit, with the understanding that the polymer chemical potential, μ_2, becomes independent of protein concentration, it is shown in Appendix A that the following condition must be satisfied:

$$\left[\frac{\partial \mu_p}{\partial \phi_2}\right]_{T,P,\phi_p} = (1-\phi_2)\left[\frac{\partial \mu_p}{\partial \phi_2}\right]_{T,\mu_1,\phi_p} \quad (2)$$

Equation 2 is a central result that is used to evaluate changes in the protein chemical potential at constant pressure from changes in the protein chemical potential occurring at constant solvent chemical potential. The latter quantity has been evaluated previously for hard-sphere systems.[40]

We present an evaluation of the protein chemical potential at constant pressure using a description of the system in terms of effective hard-sphere sizes. This approximate representation of the system is justified in view of the following considerations. First, it is emphasized that we account for the deformability and penetrability of the polymer coils (both for polymer–polymer and for polymer–protein interactions) through the careful choice of the effective hard-sphere sizes of both polymers and proteins (see section 3). Second, we realize that, in general, equations of state for simple hard-sphere systems will not be sufficient to describe complex systems such as protein–polymer mixtures. This is due to the fact that different effective hard-sphere sizes will be required to describe the polymer hard-sphere size associated with polymer–polymer interactions and that associated with polymer–protein interactions. That is, such mixtures belong to the class of so-called nonadditive hard-sphere systems.[41] However, because our aim is to describe the standard-state chemical potential of the protein in the limit of vanishing protein concentration, which is the relevant limit for the protein partitioning behavior considered here, it is not necessary to resort to equations of state for nonadditive hard-sphere systems. This follows because one can adjust the effective hard-sphere size of the protein species such that the same polymer effective hard-sphere size can be used for both polymer–polymer and polymer–protein interactions. Although, in general, this approach will not predict correctly the contribution of protein–protein interactions to the protein chemical potential, this contribution is insignificantly small in the limit of vanishing protein concentration considered in this paper. Finally, we emphasize that in our theoretical formulation the effective protein and polymer hard-sphere sizes should not be identified with the actual physical sizes of these species.

With the above considerations in mind and with the excluded-volume interactions between proteins and polymer coils, as well as between the polymer coils themselves, represented in terms of effective hard-sphere sizes, we have utilized an equation of state for a binary mixture of hard spheres at constant solvent chemical potential, as well as eq 2, to evaluate the protein chemical potential at constant pressure.[40] Under conditions of constant solvent chemical potential, Jansen et al.[40] derived the following expression for the chemical potential of component p (the protein, in our case) in a binary hard-sphere mixture of components p and 2 (the polymer in our case)

$$\left[\frac{\mu_p}{kT}\right]_{T,\mu_1} = \left[\frac{\bar{\mu}^\circ_p}{kT}\right] + \ln\left[\frac{\phi_p}{1-\xi_3}\right] + \sigma_p^3\eta_0 + 3\sigma_p^2\eta_1 + 3\sigma_p\eta_2 + 3\sigma_p^2\eta_1\eta_2 + \frac{9}{2}\sigma_p^2\eta_2^2 + 3\sigma_p^3\eta_2^3 \quad (3)$$

where the parameters η_k and ξ_k are defined by

$$\eta_k = \xi_k/(1-\xi_3) \quad (4)$$

and

$$\xi_k = \phi_2\sigma_2^{k-3} + \phi_p\sigma_p^{k-3} \quad (5)$$

where $k = 0$, 1, 2, and 3 and ϕ_2 and ϕ_p are the volume fractions of the polymer and protein, respectively. In eq 3, $(\bar{\mu}^\circ_p/kT)$ is the concentration-independent contribution to the protein chemical potential, and in eqs 3 and 5, σ_2 and σ_p are the effective hard-sphere diameters of the polymer coils and the protein molecules, respectively. Using eqs 4 and 5 in eq 3, then substituting the resulting eq 3 in eq 2, and finally integrating (in the limit of vanishing protein concentration, $\phi_p \to 0$) from $\phi_2 = 0$ to ϕ_2, we obtain the following useful result:

$$\left[\frac{\mu^\circ_{p,t}}{kT}\right] = \left[\frac{\mu_p}{kT}\right]_{T,P,\phi_2,\phi_p\to 0} - \left[\frac{\mu_p}{kT}\right]_{T,P\phi_2\to 0,\phi_p\to 0} = \frac{9}{2}r_\sigma^3 - \frac{9}{2}r_\sigma^2 + \phi_2\left[1+\frac{9}{2}r_\sigma^2\right] + \frac{\phi_2^2}{1-\phi_2}\left[3r_\sigma^3+\frac{9}{2}r_\sigma^2\right] + 3\frac{\phi_2^3}{(1-\phi_2)^2}r_\sigma^3 + \ln(1-\phi_2)(-4r_\sigma^3+6r_\sigma^2-3r_\sigma) + \frac{1}{1-\phi_2}\left[-6r_\sigma^3+\frac{9}{2}r_\sigma^2\right] + \frac{3}{2(1-\phi_2)^2}r_\sigma^3 \quad (6)$$

where $r_\sigma = \sigma_p/\sigma_2$. In eq 6, $\mu_p(T,P,\phi_2,\phi_p\to 0)$ corresponds to the protein chemical potential in a polymer solution phase having an effective hard-sphere polymer volume fraction, ϕ_2, and $\mu_p(T,P,\sigma_2\to 0,\phi_p\to 0)$ corresponds to the chemical potential of the protein in a polymer-free solvent phase. Note that the difference between these two quantities is equal to the standard-state protein chemical potential, $\mu^\circ_{p,t}/kT$, in eq 1 and in paper 1.[19]

To utilize eq 6 in eq 1, in predicting the change in the logarithm of the protein partition coefficient, $\Delta\ln K_p$, the two length scales, σ_2 and σ_p, need to be evaluated. Recall that σ_2 is the effective hard-sphere diameter of the polymer, which reflects the deformability and penetrability associated with the polymer–polymer excluded-volume interactions, and σ_p is the effective hard-sphere diameter of the protein, which reflects the deformability and penetrability associated with protein–polymer excluded-volume interactions.

3. Effective Hard-Sphere Potentials for Steric Interactions

The topic of polymer–polymer interactions in solutions of identifiable polymer coils has received considerable experimental and theoretical attention over the past few decades.[34-36,41-43] Our approach utilizes the classical theories of Flory[41] to calculate the radius of gyration of isolated polymer coils (PEO) and Flory and Krigbaum[34]

Table I
Comparison of the Predicted PEO Radius of Gyration, R_g, and Measured R_g from Neutron- and Light-Scattering Experiments[44] as a Function of PEO Molecular Weight, M_2, and the Predicted Effective Hard-Sphere Radius of PEO, R_{22}^{HS}, as a Function of M_2

M_2 (Da)	pred R_g (Å)	measd R_g (Å)	R_{22}^{HS} (Å)
3000	20.4	18.9	11.4
4000	23.9	22.6	13.8
5000	27.1	26.0	16.0
6000	29.9	29.1	18.0
7000	32.6	32.0	19.9
8000	35.1	34.7	21.7
9000	37.5	37.4	23.5
10000	39.8	39.9	25.1

to calculate the effective hard-sphere diameters corresponding to the effective excluded-volume interactions between two polymer coils. The theoretically calculated polymer-coil radius of gyration[41] is substantiated through a comparison with the radius of gyration of an isolated PEO coil obtained using neutron-scattering and light-scattering measurements.[44] To assess the validity of the characterization of polymer–polymer interactions using an effective hard-sphere potential over the range of polymer concentrations encountered in two-phase aqueous polymer systems, we have compared available vapor-pressure measurements of aqueous PEO solutions[45] with predicted vapor-pressure values based on the use of the theoretically calculated effective polymer hard-sphere diameters.

Using Flory's theory[41] and the following literature values for the physical parameters which characterize PEO in water at 25 °C, $\chi = 0.45$,[46,47] $l = 1.46$ Å,[41] $v_1° = 18$ cm^3/mol, $v_{sp} = 0.83$ cm^3/g,[48] and $c_\infty = 4.1$,[41] where χ is the Flory–Huggins interaction parameter, l^2 is the mean-square length of each bond comprising the repeat units of PEO, $v_1°$ is the molar volume of the solvent, v_{sp} is the specific volume of the polymer, and c_∞ is the characteristic ratio of the PEO chain, the radius of gyration of PEO was calculated as a function of PEO molecular weight. In Table I, the theoretically predicted PEO radius of gyration, R_g, is compared as a function of PEO molecular weight to the radius of gyration data extrapolated from neutron-scattering and light-scattering measurements for PEO in water.[44] As can be seen, a good agreement exists between the theoretical and experimental values of the polymer radius of gyration.

The Flory–Krigbaum theory[34] estimates the *effective volume* excluded by one polymer coil to another, U_2. The effective hard-sphere radius of a polymer coil characterizing polymer–polymer interactions, R_{22}^{HS}, is calculated by equating the expression for U_2 with the following well-known expression[1] for the excluded volume between two hard spheres:

$$U_2 = 32\pi(R_{22}^{HS})^3/3 \tag{7}$$

The predicted R_{22}^{HS} values as a function of PEO molecular weight, M_2, are also presented in Table I. Owing to the possible effect of polymer–polymer interactions on the average configuration of the polymer coils,[12-14] one can, in general, expect the effective hard-sphere polymer radius to exhibit a concentration dependence as the polymer concentration increases. As this aspect of the polymer-coil behavior was not incorporated in our description of the effective polymer-coil hard-sphere radius, a comparison between the measured vapor pressure of PEO in water[45] and a theoretical prediction, which explicitly incorporates the effective hard-sphere radius of the polymer, was made to assess the range of validity of our approximate treatment in terms of a concentration-independent R_{22}^{HS}.

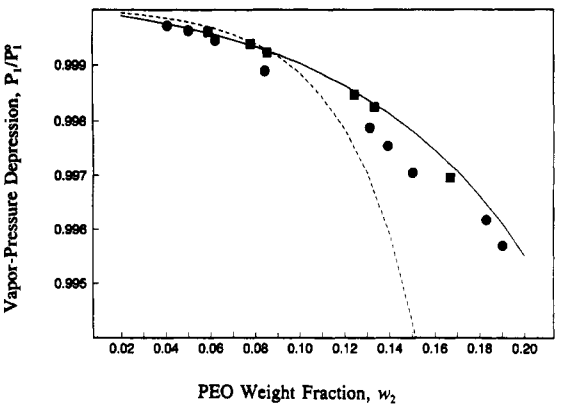

Figure 1. Comparison of predicted (lines) and experimental (data points) vapor-pressure depression, $P_1/P°_1$ of aqueous PEO solutions as a function of PEO weight fraction, w_2: 3790 Da (— and ●); 9037 Da (- - and ■).

We have computed the vapor pressure of an aqueous solution of PEO using the well-known result[49]

$$\frac{P_1}{P°_1} = e^{-V°_1\Pi/kT} \tag{8}$$

where P_1 is the vapor pressure of an aqueous PEO solution, $P°_1$ is the vapor pressure of pure water, $V°_1$ is the molecular volume of the solvent, and Π is the solution osmotic pressure. We have evaluated the osmotic pressure of the polymer solution using the Carnahan–Starling equation of state for a monodisperse hard-sphere system[32,33] This description of the polymer solution in terms of effective hard-sphere sizes is consistent with our treatment of polymer–polymer interactions in solutions of polymers *and* proteins. Accordingly, the vapor pressure of the PEO solution can be calculated as

$$\frac{P_1}{P°_1} = \exp\left[\frac{-V°_1N_2(1 + \phi_2 + \phi_2^2)}{V(1-\phi_2)^3}\right] \tag{9}$$

where N_2/V is the number density of PEO coils in the solution and ϕ_2 is the effective hard-sphere volume fraction occupied by the polymer coils in solution ($\phi_2 = 4\pi N_2(R_{22}^{HS})^3/3V$).

In evaluating the vapor-pressure depression predicted by eq 9 and subsequently comparing it with the experimental measurements reported by Haynes et al.,[45] one must consider the influence of polymer-size polydispersity in the polymer samples used in the experiments. Specifically, the PEO samples used in the vapor-pressure measurements[45] had number-average molecular weights of 3790 and 9037 Da and weight-average molecular weights of 3860 and 11 800 Da, respectively. Since the osmotic pressure of a polydisperse system reflects the number-average properties,[49] in computing the effective hard-sphere radius of the polymer coils the number-average molecular weights were used. From Table I, an interpolation of the appropriate molecular weights to 3790 and 9037 Da yields effective PEO hard-sphere radii (R_{22}^{HS}) of 13.5 and 23.5 Å, respectively. In Figure 1, the predicted vapor-pressure depression of the aqueous PEO solutions, $P_1/P°_1$, as a function of polymer weight fraction, w_2, is compared to experimental measurements. For the PEO sample corresponding to a number-average molecular weight of 3790 Da, the reasonable agreement between the calculated (solid line) and experimental (●) vapor pressures of the PEO solutions shown in Figure 1 suggests that the essential nature of the polymer–polymer inter-

actions has been captured effectively. Unfortunately, scatter in the experimental data points prevents a more precise comparison between the theoretical predictions and experimental measurements of the vapor-pressure depression. However, the general agreement suggests that such a description of the polymer–polymer interactions will provide a reasonable estimation for their contribution to the protein standard-state chemical potential and associated protein partition coefficient. For the larger PEO having a molecular weight of 9037 Da, the comparison of theory (dashed line) and experiment (■) shown in Figure 1 indicates that a significant difference exists beyond PEO weight fractions of approximately 0.1. This difference may reflect the transition in the underlying structure of the PEO solution, from one composed of singly-dispersed polymer coils to one characterized by an entangled mesh of polymer coils, that can occur with either increasing PEO weight fraction or molecular weight.[3] Significantly, and as reported[19] in paper 1, aqueous solutions of PEO having a molecular weight of approximately 10 000 Da will undergo such a transition in the vicinity of a PEO weight fraction of approximately 0.1. With this in mind, it is very reasonable to suggest that our description of the 9037-Da PEO solution as one composed of separate polymer coils becomes inappropriate above PEO weight fractions of around 0.1. PEO of molecular weight 3790 Da undergoes a similar transition in nature, but at a significantly higher PEO weight fraction of approximately 0.2 (or more). In summary, over the range of solution conditions consistent with the description of the aqueous PEO solution as one containing singly-dispersed polymer species, the agreement between the theoretical predictions and the experimental vapor-pressure measurements is very reasonable. It is noteworthy that this conclusion is supported by neutron-scattering measurements which will be reported in a subsequent paper of this series.[50]

The second important type of interaction that must be characterized to predict the protein chemical potential in aqueous PEO solutions is the direct polymer–protein interaction. First, we consider excluded-volume interactions occurring between the protein and the polymer, and subsequently, in section 5, we consider the influence of other interactions (attractions). The steric interaction in this case is rather more interesting than the polymer–polymer one described earlier, since it involves two unlike species: a rather flexible, deformable and penetrable polymer coil, and a relatively impenetrable, globular and structured protein molecule. At Θ-solvent conditions for the polymer, where the configurations of a polymer chain can be described in analogy with Brownian motion, the solution of the diffusion equation yields the following analytical expression for the excluded volume arising from the interaction of a flexible chain and an impenetrable sphere:[51]

$$U_p = 4\pi R_p R_g^2 + 8\pi^{1/2} R_p^2 R_g + 4\pi R_p^3/3 \qquad (10)$$

Equation 10 is not strictly applicable in the case of PEO in water, where solution conditions at 25 °C are better (good solvent) than Θ-solvent conditions,[44,46-48] since additional correlations between polymer segments will influence the nature of the excluded-volume interaction between the entire polymer coil and the protein. However, consideration of this equation proves illuminating since some qualitative features of the equation are common to the two cases of Θ-solvents and good solvents. In particular, from an inspection of eq 10, it can be seen that when the polymer coil is much larger than the protein, that is, $R_g \gg R_p$, the excluded volume scales as $R_p R_g^2$. This contrasts to the opposite limit where $R_p \gg R_g$ and the excluded volume scales as R_p^3. The different functional forms of U_p in the two limits, $R_p \ll R_g$ and $R_p \gg R_g$, reflects the difference in the deformability and penetrability of the protein as compared to the polymer. It is this feature of the interaction that we have attempted to capture in our evaluation of the protein–polymer excluded volume away from the Θ-solvent conditions. To account for the swelling of the PEO chains, which arises from the interactions between PEO segments in the same coil, a simple Monte Carlo method was developed to estimate this excluded-volume contribution.[37-39] Although qualitatively one may expect the excluded volume to be similar to that corresponding to the Θ-solvent case, the purpose of the present work is to provide a somewhat more quantitative determination of the protein chemical potential in a polymer solution. Accordingly, the steric interaction between the polymer coil and the protein was evaluated using a reptation method[37] to generate the configurations of the polymer coil (on a cubic lattice) in the vicinity of the protein (modeled as a hard sphere or ellipsoid). The excluded volume is evaluated as[38,39]

$$U_p = V^\circ_p \left[\frac{N}{\langle m \rangle}\right] \qquad (11)$$

where N is the number of statistical polymer segments per polymer coil, V°_p is the molecular volume of the protein, and $\langle m \rangle$ is the number of statistical polymer segments which simultaneously overlap the protein volume, averaged over an ensemble of polymer-coil configurations generated using the Monte Carlo method. Equation 11 can be understood intuitively using the following simple argument. If all N statistical polymer segments on the chain interact *independently* with the protein, the excluded volume, U_p, would be equal to NV°_p (the polymer segment volume is very small compared to the protein volume).[1] However, the polymer segments are not independent since they belong to the same polymer chain, and, therefore, their positions are correlated. The consequence of the polymer chain connectivity is that if a single polymer segment interacts with the protein, because it belongs to a polymer coil, there will be, in all likelihood, other polymer segments interacting simultaneously with the protein. This implies a *reduction* of the excluded volume NV°_p by the factor $\langle m \rangle$. In addition to providing a quantitative evaluation of the excluded volume, an additional advantage of this general method is that it is not constrained to linear polymer architectures or spherical protein geometries. An account of nonspherical (ellipsoidal) protein geometries will also be given in this paper.

To ensure the correct generation of an unbiased sample of polymer configurations, as shown in Figure 2, the root-mean-square end-to-end length of the polymer coil, $\langle R^2 \rangle^{1/2}$, was evaluated as a function of the number of polymer-coil segments, N. The data points represent the average of 10 independent runs, each consisting of $200N^2$ attempted polymer-segment moves, and the error bars extend a standard deviation on either side of the average. The dashed line in Figure 2 is a linear fit to the data points and was used to determine the exponent relating $\langle R^2 \rangle^{1/2}$ to N. The value determined was 0.587 ± 0.018 and is consistent with the expected value of approximately $^3/_5$ for a self-avoiding polymer coil in three dimensions.[2,3]

To determine the scaling prefactor that relates the dimensions of the lattice-generated polymer coil to the actual size of the PEO coils in aqueous solution, a correspondence between the size of a lattice segment and a PEO segment (a) must be established. In essence, the number of bonds along the PEO chain that corresponds

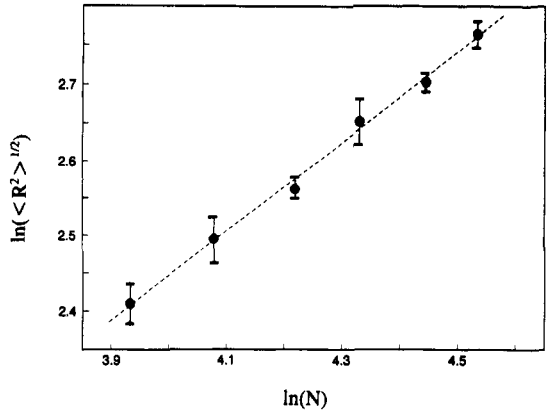

Figure 2. Logarithm of the root-mean-square end-to-end length of a polymer coil, ln ($\langle R^2 \rangle^{1/2}$), as a function of the logarithm of the number of polymer segments per coil, ln (N). The error bars extend one standard deviation on either side of the mean value, and the line of best fit is shown.

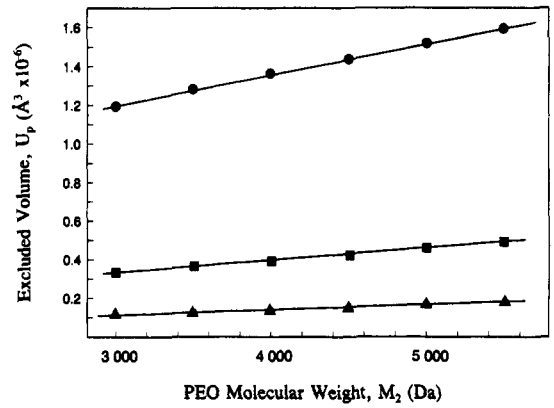

Figure 3. Predicted excluded volume of polymer and protein, U_p, as a function of PEO molecular weight, M_2: (▲) cytochrome c, R_p = 19 Å; (■) ovalbumin, R_p = 29 Å; (●) catalase, R_p = 52 Å.

to the statistical-segment size is determined by the polymer flexibility, that is, by c_∞.[41] Consistent with the known flexibility of PEO (c_∞ = 4.1),[41] we assume that four bonds of the PEO chain constitute one statistical segment of the simulated polymer chain. Accordingly, the number of statistical polymer segments within the polymer chain is given by $N = n/c_\infty$. The size of a statistical segment was determined by requiring that the radius of gyration of the statistical chain (with N polymer segments) equals the radius of gyration of the PEO chain. In order for the dimensions of the simulated chains (see Figure 2) to equal the measured PEO chain dimensions (Table I), a statistical-segment length corresponding to 4 Å was determined. Note that although the solvent condition for PEO in water does not correspond to the athermal conditions of the simulation, the departure of the solvent conditions from athermal is incorporated by choosing the effective statistical-segment size to be 4 Å.[3]

The excluded volume characterizing the polymer–protein interactions, evaluated according to eq 11, is presented in Figure 3 as a function of PEO molecular weight. The results are presented for three spherical protein sizes, corresponding to cytochrome c (R_p = 19 Å), ovalbumin (R_p = 29 Å), and catalase (R_p = 52 Å), for the range of PEO molecular weights between 3000 and 5500 Da. From an inspection of Figure 3 it can be seen that the excluded volume increases both with protein size and with PEO molecular weight.

Using the excluded-volume data presented in Figure 3 and the spherical (physical) size of a protein, the effective hard-sphere radius of the polymer coil (associated with excluded-volume interactions with a protein), R_{2p}^{HS}, can be evaluated from[1]

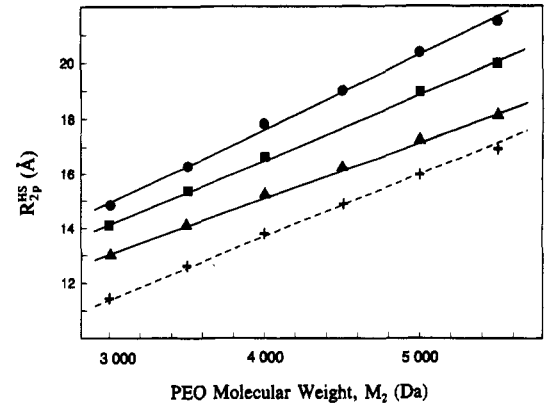

Figure 4. Predicted effective hard-sphere radius of a PEO coil, R_{2p}^{HS}, associated with the excluded-volume interaction with a protein as a function of PEO molecular weight, M_2: (▲) cytochrome c, R_p = 19 Å; (■) ovalbumin, R_p = 29 Å; (●) catalase, R_p = 52 Å. Also shown is the effective hard-sphere radius of a PEO coil, R_{22}^{HS}, associated with the excluded-volume interaction with another polymer coil having the same molecular weight (+).

$$U_p = \frac{4\pi}{3}(R_p + R_{2p}^{HS})^3 \qquad (12)$$

The predicted variation of R_{2p}^{HS} with PEO molecular weight is shown in Figure 4. Owing to the deformable and penetrable nature of the polymer coil, R_{2p}^{HS} increases both with the size of the protein molecule and with the polymer molecular weight. The first trend reflects the fact that, with an increase in the protein size, there will be a decrease in the number of polymer configurations which permit the protein to penetrate the volume occupied, on average, by the polymer coil. Furthermore, for a fixed protein size, as is also reflected in Figure 4, an increase in polymer molecular weight results in an increase in the effective hard-sphere radius of the PEO coil. For small proteins, the increase in the effective polymer size is less than for the large proteins. This is, once again, because the fraction of the average polymer volume which is accessible to the protein increases with decreasing protein size. In Figure 4, for the purpose of comparison, we also show the effective hard-sphere radius of a PEO coil associated with polymer–polymer interactions, R_{22}^{HS} (taken from Table I). It is interesting to observe that $R_{22}^{HS} < R_{2p}^{HS}$. In other words, for the range of protein sizes investigated, the polymers are more permeable to each other than to the protein species.

While the above discussion of R_{2p}^{HS} illuminates the nature of polymer–protein interactions, it is necessary to further develop the above result to incorporate the protein–polymer and polymer–polymer potentials into a thermodynamic framework which can predict the standard-state protein chemical potential. In section 3 we developed a generalized hard-sphere representation of the polymer–protein solution, and, in so doing, we implicitly assumed the same polymer coil effective hard-sphere size to describe both polymer–polymer and polymer–protein interactions. The essential complication arises from the fact that, as reported in Figure 4, different effective hard-sphere polymer sizes are required to describe polymer–polymer interactions (R_{22}^{HS}) and polymer–protein interactions (R_{2p}^{HS}). However, with a change in polymer molecular weight, rather than attributing the change in the protein–polymer excluded volume to a change in the effective hard-sphere size of the polymer (R_{2p}^{HS}), one can distribute the change between an effective hard-sphere protein size and an effective hard-sphere polymer size. For our purposes

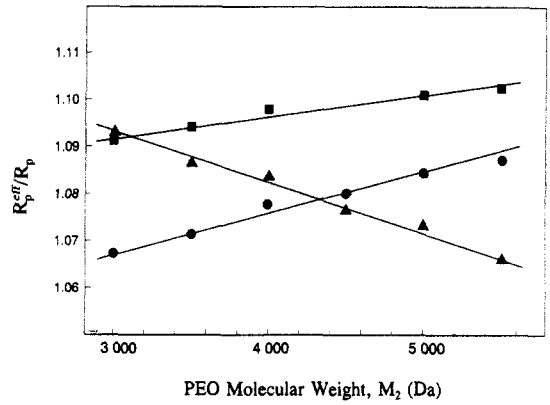

Figure 5. Predicted ratio of the effective hard-sphere protein and physical protein radii, R_p^{eff}/R_p, as a function of PEO molecular weight, M_2: (▲) cytochrome *c*, R_p = 19 Å; (■) ovalbumin, R_p = 29 Å; (●) catalase, R_p = 52 Å.

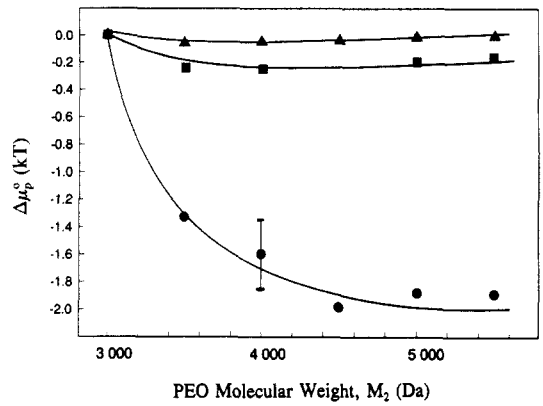

Figure 6. Predicted standard-state protein chemical potential in a 10% w/w aqueous PEO solution relative to that in a solution of PEO 3000 Da, $\Delta\mu^\circ_p$, as a function of PEO molecular weight, M_2: (▲) cytochrome *c*, R_p = 19 Å; (■) ovalbumin, R_p = 29 Å; (●) catalase, R_p = 52 Å. The error bars extend one standard deviation on either side of the mean value.

it is advantageous to use the same polymer effective hard-sphere radius to characterize the polymer for both protein–polymer and polymer–polymer interactions, that is, R_{22}^{HS} (since this is required for the thermodynamic analysis). Accordingly, using the excluded volumes calculated from eq 12, with R_{2p}^{HS} taken from Figure 4, and the effective hard-sphere radii of the polymer coils that characterize the polymer–polymer interactions (R_{22}^{HS}) from Table I, an effective hard-sphere radius of the protein molecules, R_p^{eff}, can be evaluated by rewriting eq 12 in the form

$$U_p = \frac{4\pi}{3}(R_p^{eff} + R_{22}^{HS})^3 \qquad (13)$$

The ratio of the effective protein size to the actual protein size, R_p^{eff}/R_p, evaluated according to the above description, as a function of PEO molecular weight is presented in Figure 5, where it is evident that the protein size used in eq 13 is a function of the polymer molecular weight. These predictions follow naturally from the results presented in Figure 4, and the definition of R_p^{eff}/R_p, namely, $R_p^{eff}/R_p = 1 + (R_{2p}^{HS} - R_{22}^{HS})/R_p$. Note that below we identify R_{22}^{HS} with $\sigma_2/2$ and R_p^{eff} with $\sigma_p/2$ in eq 6 in order to evaluate the thermodynamic properties of the system. For a small protein like cytochrome *c*, an increase in PEO molecular weight results in a decrease in the effective protein radius and may be understood in terms of the increase in R_{2p}^{HS}, relative to R_{22}^{HS}, seen in Figure 4. Physically, as a function of increasing PEO molecular weight, the penetrability of the polymer coil toward the small protein causes R_{2p}^{HS} to increase more slowly than R_{22}^{HS}. Perhaps a less expected result is the observed increase in the effective protein radius with PEO molecular weight observed for the large proteins. For large proteins, such as catalase, the effective hard-sphere size of the polymer used to characterize the protein–polymer interactions (R_{2p}^{HS}) is more sensitive to polymer molecular weight (increases more rapidly) than is the effective hard-sphere size of the polymer coil used to characterize the polymer–polymer interactions (R_{22}^{HS}). This arises from the fact that the polymer coils are less penetrable to the large proteins, as can be seen from a careful inspection of Figure 4.

It should always be kept in mind that the effective hard-sphere size of the protein used in eq 6 for the protein chemical potential reflects the nature of both protein–polymer and polymer–polymer interactions. Clearly, this approach will only be successful in the limit of vanishing protein concentration, where interactions between proteins have a negligible effect on the protein chemical potential.

4. Evaluation of the Standard-State Protein Chemical Potential

To evaluate the standard-state protein chemical potential using the effective hard-sphere sizes evaluated in section 3, as indicated above, we identify R_{22}^{HS} with $\sigma_2/2$ and R_p^{eff} with $\sigma_p/2$ in eq 6. Figure 6 presents a prediction of the change in the standard-state protein chemical potential, $\Delta\mu^\circ_p$, as a function of PEO molecular weight, M_2, for three proteins of differing size and for solution conditions corresponding to 10% w/w PEO in water (as discussed in paper 1, this PEO concentration is typical to that encountered in the top PEO-rich phase of a two-phase aqueous polymer system containing PEO and dextran).[19] For the smallest protein species, cytochrome *c* (▲), a negligible change in the standard-state protein chemical potential is predicted to accompany changes in PEO molecular weight from 3000 to 5500 Da, subject to the statistical uncertainty introduced by the evaluation of the protein–polymer excluded volume using the Monte Carlo method. The change in the chemical potential is amplified by the protein size. For example, the prediction for the change in the standard-state chemical potential of catalase (●) shows a statistically significant decrease with an increase in PEO molecular weight. On the basis of eq 1, it is evident that this decrease in the standard-state protein chemical potential translates into a predicted increase in the protein partition coefficient with increasing PEO molecular weight. This reuslt is in direct contrast to the trends observed experimentally, where increasing PEO molecular weight resulted in a decrease in the protein partition coefficient.[22,23] Therefore, within the approximations of the thermodynamic formulation presented in this paper, it appears that on the basis of entropy alone (steric interactions) it is not possible to account for the observed partitioning behavior of proteins in the PEO–dextran two-phase aqueous polymer system.

One approximation in the above treatment is the representation of the protein molecules as spherical bodies. Indeed, many proteins are rather more ellipsoidal in shape with ratios of the major and minor axes of approximately 3.[52,53] To assess the role of the more detailed protein geometry on the partitioning behavior, we have investigated the influence of introducing asymmetry in the protein shape. The Monte Carlo method developed for the evaluation of the protein–polymer interactions is well suited for this investigation, and geometries more intricate than ellipsoidal ones could also be treated readily.

Figure 7 shows the influence of the protein shape on the

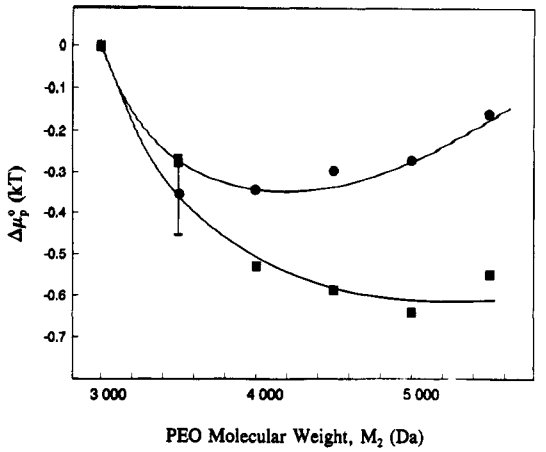

Figure 7. Predicted effect of protein shape asymmetry on the standard-state protien chemical potential in a 10% w/w aqueous PEO solution relative to that in a solution of PEO 3000 Da, $\Delta\mu^\circ_p$, as a function of PEO molecular weight, M_2. The protein volume corresponds approximately to that of bovine serum albumin: (■) sphere with radius of 35 Å; (●) ellipsoid with a semimajor axis of 79 Å and a semiminor axis of 23 Å. The error bars extend one standard deviation on either side of the mean value.

change in the standard-state protein chemical potential, $\Delta\mu^\circ_p$, predicted to accompany a change in PEO molecular weight, M_2. Keeping the volume of the protein constant (which, for the sake of illustration, corresponds to the volume of a BSA molecule), the aspect ratio of the protein was increased from 1.0 (■) to 3.5 (●).[52,53] Interestingly, it appears that an increase in the asymmetry of the protein will increase (less negative) the change in the standard-state protein chemical potential. Physically, this arises because an increase in the aspect ratio of the protein causes an increase in the magnitude of the excluded volume characterizing the protein–polymer interactions. The relatively large magnitude of this effect, as seen in Figure 7, suggests that, for a more accurate and quantitative prediction of protein partitioning in two-phase aqueous polymer systems, it will be necessary to account for the nonspherical shape of most proteins. Furthermore, the predicted influence of the protein shape on the standard-state protein chemical potential suggests that protein partitioning should be sensitive to changes in the conformational states of proteins.

5. Attractions and the Standard-State Protein Chemical Potential

In paper 1, in addition to revealing the (competing) contributions of steric protein–polymer and polymer–polymer interactions to the standard-state protein chemical potential, the important role of weak short-ranged attractive interactions between the protein and the polymer segments was examined.[19] For this purpose, qualitative scaling-type arguments were used. The conclusion of that investigation was that weak attractive interactions influence the standard-state protein chemical potential in a manner which is consistent with trends observed experimentally. The primary aims of this section are (1) to assess the validity of the scaling-type arguments through a simple Monte Carlo calculation and (2) to determine the strength of attractive interactions that would be sufficient to account for the experimentally observed influence of PEO molecular weight on the protein partition coefficient.

The treatment of the attractive interactions between the protein and the polymer-coil segments utilizes a hard-sphere perturbation approach,[31] which has been successful in describing the influence of weak attractions on the equilibrium phase behavior and light-scattering properties of other colloidal systems.[40,54,55] This approach relies on the fact that, for systems with weak interactions, the attractive contribution to the osmotic pressure remains of order ρ^2, where ρ is the number density of a species in solution, up to quite high number densities.[40,54,55] To second order in number density, the osmotic pressure, Π, for a solution containing a mixture of species can then be written as[31]

$$\Pi = \Pi_{Hs} + \sum_{ij} B_{ij}^{att} \rho_i \rho_j \tag{14}$$

where Π_{HS} is the hard-sphere contribution to the osmotic pressure, ρ_i is the number density of species i, and B_{ij}^{att} is the attractive portion of the second virial coefficient for species i and j, defined as

$$B_{ij}^{att} = {}^1/_2 \int (1 - e^{-V_{ij}^{(1)}(r)})\, d^3r \tag{15}$$

where $V_{ij}^{(1)}(r)$ is the contribution of the attractive interaction to the potential of mean force between species i and j which are separated by a distance r. In the notation of statistical mechanical perturbation theory, $V_{ij}^{(1)}(r)$ is the perturbation potential relative to a reference system (which, in our case, is the pure hard-sphere system treated in sections 3 and 4).

Under the constraint of constant solvent chemical potential, the contribution of attractive interactions of the form given in eq 14 to the standard-state chemical potential of species i in a mixture of other species j is given by[40]

$$[(\mu^\circ_i)^{att}/kT]_{\mu_1} = 2\sum_j B_{ij}^{att} \rho_j \tag{16}$$

For a mixture of proteins (species p) and polymers (species 2) dispersed in a solvent (species 1) at vanishing protein concentration ($\rho_p \to 0$), eq 16 for i = p reduces to

$$[(\mu^\circ_p)^{att}/kT]_{\mu_1} = 2B_{2p}^{att} \rho_2 \tag{17}$$

Recall that the solvent, species 1, does not appear explicitly in eq 17 since it is treated in the continuum approximation. However, the solvent properties *do* influence the protein chemical potential; that is, B_{2p}^{att} is a function of the solvent quality, since all interactions in the solution are mediated by the solvent. It is interesting to note that the expression in eq 17 is identical to that derived in paper 1.[19] Here, however, we wish to evaluate the protein chemical potential at constant pressure (rather than at constant solvent chemical potential; see Appendix A). This can be achieved readily by combining eq 2, which relates changes in the chemical potential at constant pressure to those at constant solvent chemical potential, and eq 17, which describes the influence of the attraction on the protein chemical potential at constant solvent chemical potential. The resulting expression for the contribution of the attractive interactions to the standard-state protein chemical potential at constant pressure is given by[40]

$$[(\mu^\circ_p)^{att}/kT]_P = 2B_{2p}^{att} \rho_2 - B_{2p}^{att} V_2 \rho_2^2 \tag{18}$$

where $V_2 = 4\pi(R_{22}^{HS})^3/3$.

Whereas in paper 1 the attractive contribution to the second virial coefficient, B_{2p}^{att}, was estimated using simple scaling-type arguments, here we report a more quantitative evaluation using a Monte Carlo method. Since B_{2p}^{att} describes the interactions between a deformable and penetrable polymer coil and an impenetrable sphere, the evaluation of this quantity requires that we account for the influence of both repulsive excluded-volume and attractive interactions on the configurations that are

sampled by the polymer coil when residing in the vicinity of the protein. We approximate this evaluation by the integral

$$B_{2p}^{att} = {}^1/_2\langle \int_0^\infty (1 - e^{-V^{(1)}_{2p}(r)/kT})\, d^3r \rangle \approx {}^1/_2 \int_0^\infty (1 - e^{-\langle V^{(1)}_{2p}(r)/kT \rangle})\, d^3r \quad (19)$$

where the angular brackets denote a weighted average over all possible polymer configurations that (i) do not intersect the volume occupied by the protein and (ii) satisfy the constraint that the centers of mass of the polymer coil and the protein be separated by a distance r. To evaluate B_{2p}^{att} we have used the approximation presented in eq 19, where the averaging is performed over the interaction potential, rather than over the entire integral. This approximation, which greatly reduces the effort involved in evaluating the integral, is a good one provided that $|V^{(1)}_{2p}(r)/kT| \ll 1$. We have assessed the validity of this approximation using the theory of Barker and Henderson[60] to estimate the size of the term of order $(V^{(1)}_{2p}(r)/kT)^2$. For a spherical colloid having a radius of 37 Å (the radius of bovine serum albumin), a polymer chain with 147 statistical segments (the size of PEO 8650 Da), and $\epsilon \leq 0.1$, the truncation error was less than 20%. For the smaller PEO molecular weights investigated in the remainder of this paper the truncation error will be less. For a short-ranged contact-type interaction between the polymer-coil segments and the protein (as was treated in paper 1 and is investigated here), this average can be simply evaluated as

$$-\frac{\langle V^{(1)}_{2p}(r) \rangle}{kT} = \frac{\sum^{\{C\}} m_s \epsilon e^{m_s \epsilon}}{\sum^{\{C\}} e^{m_s \epsilon}} \quad (20)$$

where the summations are over a representative sample of the polymer configurations, {C}, such that the two criteria mentioned above are satisfied, m_s is the number of contacts between the polymer-coil and the protein for a given polymer-coil configuration, and ϵ is the energy change upon bringing a polymer-coil segment from infinity to the protein surface (ϵ is measured in units of kT and is defined to be positive for an attractive interaction). In view of the conditions for which the perturbation approach is valid, that is, for weak long-ranged attractions,[31,40,54,55] it is interesting to note that, despite the short-ranged attractive nature of the interactions between the polymer *segments* and the protein, the interaction potential between the polymer *coil* and the protein, as evaluated in eq 20, is slowly varying and long-ranged. Finally, it is relevant to mention that the above framework is also suitable for exploring the influence of different types of interaction potentials on the predicted protein partitioning behavior.

In Figure 8, the contribution of the attractive interactions between the polymer-coil segments and the protein to the standard-state protein chemical potential at constant pressure, evaluated according to eqs 18–20, is presented as a function of PEO molecular weight, M_2. The quantity reported is the change in the attractive contribution to the standard-state protein chemical potential, $(\Delta\mu^\circ_p)^{att}$, accompanying an increase in PEO molecular weight, M_2, for a fixed protein size corresponding to that of ovalbumin (R_p = 29 Å) and three different interaction energies (ϵ = 0.001, 0.01, and 0.1 kT). It is evident that an increase in PEO molecular weight results in an increase in the chemical potential of the protein and

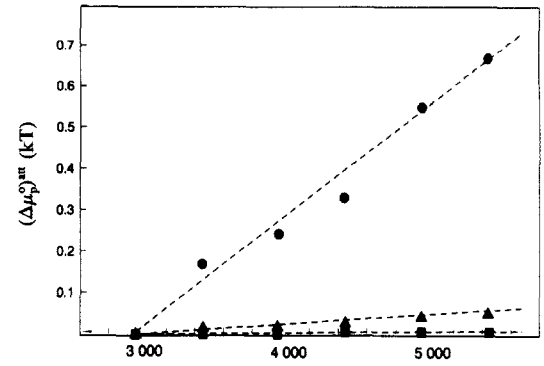

Figure 8. Predicted contribution of the protein–polymer attraction to the standard-state protein chemical potential in a 10% w/w aqueous PEO solution relative to a solution of PEO 3000 Da, $(\Delta\mu^\circ_p)^{att}$, as a function PEO molecular weight, M_2, for ovalbumin (R_p = 29 Å). Polymer segment–protein interaction energies ϵ (in units of kT): (■) 0.001; (▲) 0.01; (●) 0.1.

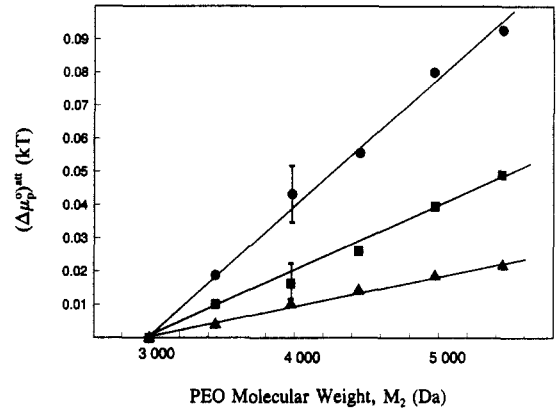

Figure 9. Predicted contribution of the protein–polymer attraction to the standard-state protein chemical potential in a 10% w/w aqueous PEO solution relative to a solution of PEO 3000 Da, $(\Delta\mu^\circ_p)^{att}$, as a function PEO molecular weight, M_2. Polymer segment–protein interaction energy ϵ = 0.01 (in units of kT): (▲) cytochrome c, R_p = 19 Å; (■) ovalbumin, R_p = 29 Å; (●) catalase, R_p = 52 Å. The error bars extend one standard deviation on either side of the mean value.

that the increase is mangified by the strength of the attractive interaction. Figure 9 illustrates the influence of protein size on $(\Delta\mu^\circ_p)^{att}$ with an increase in PEO molecular weight. For the three spherical proteins investigated (R_p = 19, 29, and 52 Å), the effect of protein size is also to magnify the change in $(\Delta\mu^\circ_p)^{att}$. Using eq 1, it can be seen that the predicted increase in the standard-state protein chemical potential translates into a decrease in the protein partition coefficient with an increase in PEO molecular weight. This prediction is consistent with experimental investigations of protein partitioning in the two-phase aqueous PEO–dextran system, which found that the influence of an increase in PEO molecular weight is to decrease the protein partition coefficient.[19,22,23]

The numerical evaluations of the influence of attractive interactions on the standard-state protein chemical potential can be compared to the result of the simple scaling argument reported in paper 1.[19] In particular, for the condition $R_p \approx R_g$, it was reported that[19]

$$\left[\frac{\mu^\circ_p}{kT}\right]^{att} \sim -\frac{\epsilon a R_p^2}{N^{3/5}} \quad (21)$$

and for higher molecular weights, where $R_g > R_p$, the N exponent was predicted to decrease to zero.[19] For comparison, our numerical results for ovalbumin predict an N exponent of 0.45 ± 0.05 for ϵ = 0.001 as well as ϵ = 0.01,

Table II
Predicted Contributions of Steric Repulsions, B_{2p}^{HS}, and Attractions, B_{2p}^{att}, to the Second Virial Coefficients of PEO and Ovalbumin (R_p = 29 Å) as a Function of PEO Molecular Weight, M_2, and Strength of Attraction, ϵ

M_2 (Da)	ϵ (kT)	B_{2p}^{HS} (Å^3)	$-B_{2p}^{att}$ (Å^3)	$-B_{2p}^{att}/B_{2p}^{HS}$
3000	0.01	167 500	4 940	0.03
3500		182 800	5 430	0.03
4000		199 400	6 050	0.03
4500		216 200	6 400	0.03
5000		230 900	6 610	0.03
5500		246 000	6 790	0.03
3000	0.10	167 500	76 050	0.45
3500		182 800	83 490	0.46
4000		199 400	93 920	0.47
4500		216 200	101 730	0.47
5000		230 900	104 580	0.45
5500		246 000	109 000	0.44

and 0.40 ± 0.05 for ϵ = 0.10, and, therefore, are in agreement with the simple scaling theory.[19] Very similar exponents were determined for two other protein sizes, corresponding to cytochrome c (R_p = 19 Å) and catalase (R_p = 52 Å).

Combining the contributions of both the excluded-volume interactions (see section 2) and attractive interactions (described above) to the predicted standard-state protein chemical potential for ovalbumin, it was determined that an attractive interaction of strength between 0.01 and 0.05 kT per polymer segment can predict the experimentally observed change in the protein partition coefficient with PEO molecular weight. For catalase an attractive interaction of approximately 0.20–0.30 kT is required, and for cytochrome c an attractive interaction of only (approximately) 0.01 kT is needed. Thus, on the basis of this theory, it appears that there may be a correlation between the size of the protein and the strength of the attractive interaction required to account for the change in the protein chemical potential with PEO molecular weight. This observation is suggestive of an attractive interaction between the polymer segments and the entire protein molecule, where the polymer segments are interacting with the bulk of the protein instead of solely with its surface. Van der Waals-type interactions are of this nature,[56] although it is not clear that they are of sufficient strength to explain the partitioning of the larger proteins, for example, catalase. Although the precise origin of the attractive interactions is unknown, it is interesting to note that their magnitudes are consistent with neutron-scattering measurements of BSA in aqueous PEO solutions which are reported in a companion publication.[50] Finally, it is relevant to consider the relative contributions of the attractions and the steric repulsions to the total interaction between the protein and the polymer. In Table II, the two contributions, B_{2p}^{HS} and B_{2p}^{att}, to the second virial coefficient describing the protein (ovalbumin, R_p = 29 Å)–PEO interactions are presented as a function of PEO molecular weight for ϵ = 0.01 and 0.1 kT. From the comparison presented in Table II it is evident that, despite the presence of the attractive interaction, the *net* interaction between the protein and the polymer is strongly repulsive. For an attractive interaction of around $\epsilon = 0.05kT$ (the approximate strength of attraction required to predict the partitioning behavior of ovalbumin), interpolation of the results for ϵ = 0.01 and 0.1 kT suggests that the second virial coefficient is approximately 80% of the value calculated for purely steric interactions.

6. Discussion

In section 3, we evaluated the effective hard-sphere radius of a PEO coil, R_{2p}^{HS}, needed to describe the steric interaction of a PEO coil with a globular protein molecule. Specifically, in evaluating R_{2p}^{HS}, we accounted for the increase in the penetrability of the coil to the protein as the PEO molecular weight is increased. Consequently, this approach contrasts with previous descriptions of polymer–colloid interactions in which the polymer-coil radius of gyration, R_g, was used to describe the steric interaction of a flexible polymer and a rigid colloid.[25-30] To assess the importance of taking into account the penetrability of the PEO coil, we present in Figure 10 a prediction of $\Delta\mu^\circ_p$(ovalbumin, R_p = 29 Å), calculated as a function of PEO molecular weight, using both R_g and R_{2p}^{HS} to characterize the polymer in the evaluation of the protein–polymer interactions. From an inspection of Figure 10, it can be seen that *qualitatively* different trends in the standard-state protein chemical potential are predicted. The characterization of the polymer–protein interaction using the polymer-coil radius of gyration, R_g, is seen to predict a pronounced *increase* in the standard-state protein chemical potential as a function of polymer molecular weight. In contrast, when the protein–polymer interaction is characterized using R_{2p}^{HS} (see section 3), an overall *decrease* in the protein standard-state chemical potential is predicted. The difference between the two predictions arises because the former characterization of the polymer coil does not take into account correctly the increase in the penetrability of the polymer coil (to the protein) as the polymer molecular weight is increased. This comparison demonstrates the importance of accounting for the penetrability of the polymer coil in order to describe correctly the thermodynamic properties of solutions containing globular proteins and flexible polymer coils.

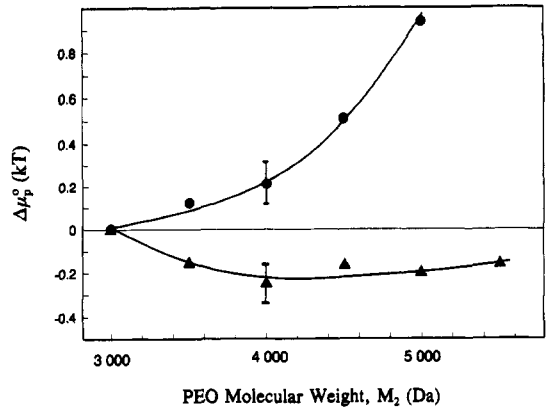

Figure 10. Predicted change in the standard-state protein chemical potential in a 10% w/w aqueous PEO solution relative to a solution of PEO 3000 Da, $\Delta\mu^\circ_p$, as a function of PEO molecular weight, M_2, for ovalbumin (R_p = 29 Å, ϵ = 0): (●) protein–polymer interaction characterized by R_g; (▲) protein–polymer interaction characterized by R_{2p}^{HS}. The error bars extend one standard deviation on either side of the mean value.

In section 2, a theoretical framework to determine the chemical potential of a protein in a polymer solution phase was presented for the conditions of constant solution temperature and pressure. In view of the previous evaluation of the protein chemical potential at constant solvent chemical potential[19] (paper 1), it is pertinent to examine to what extent these different thermodynamic ensembles can influence the predicted protein partitioning behavior. Physically, the two approaches for the evaluation of the protein chemical potential differ as follows. In paper 1, an ensemble at constant temperature and volume was used, and, accordingly, upon introduction of the protein species into the system (at constant system volume) a change in the pressure of the system occurs.[19] In the context of the formulation used to evaluate the protein chemical potential, this pressure change, which manifests itself as a

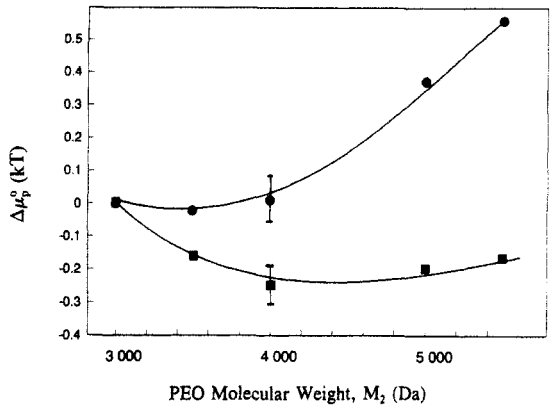

Figure 11. Comparison of the predicted standard-state protein chemical potential in a 10% w/w aqueous PEO solution relative to a solution of PEO 3000 Da, $\Delta\mu^\circ_p$ at constant pressure (■) and at constant solvent chemical potential (●) as a function of PEO molecular weight, M_2, for R_p = 29 Å and ϵ = 0. The error bars extend one standard deviation on either side of the mean value.

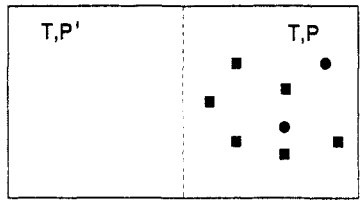

Figure 12. Diagram of an imaginary cell divided by a membrane (dashed line) which partitions a pure solvent compartment (left compartment) from a compartment containing solvent and two types of solute macromolecular species, polymers (■) and proteins (●).

change in the molar and excluded volumes of the species in the system, was neglected.[19] This approximation is equivalent to the evaluation of the protein chemical potential in a solution where the chemical potential of the solvent remains constant upon the introduction of the protein species. Although this neglect of the pressure change would appear to become negligible as the size of the system is made arbitrarily large (and vanishes as $1/L$, where L is a measure of the system size), in evaluating the chemical potential of the protein, we actually evaluate the change in the free energy of the entire system (that is, we integrate over all L), such that the effect of the pressure change does not vanish.[49] In this paper, we have made no such approximations and have derived the protein chemical potential at constant T and P. To assess the practical significance of the current development, in Figure 11, $\Delta\mu^\circ_p$ of a spherical protein (R_p = 29 Å) at constant solvent chemical potential and at constant pressure is presented as a function of PEO molecular weight. It is apparent that, for the prediction of rather subtle changes in the protein chemical potential, the two approaches can lead to rather different predictions of the protein chemical potential. Note that the quantities being compared in Figure 11 are $\mu_p(\phi_2,\phi_p\to0,T,\mu_1) - \mu_p(\phi_2\to0,\phi_p\to0,T,\mu_1)$ and $\mu_p(\phi_2,\phi_p\to0,T,P) - \mu_p(\phi_2\to0,\phi_p\to0,T,P)$. It is apparent that the change in the protein chemical potential at constant T and μ_1 is always greater than that at constant T and P. This difference can be understood with reference to the imaginary experiment presented in Figure 12 (see also Appendix A). A process involving the introduction of a species into the right compartment of the cell at constant solvent chemical potential will result in a higher pressure ($P + \Pi$) within the right compartment as compared to the same process conducted at constant P. In the latter case, following the introduction of impermeable solutes into the right compartment there will be a decrease in the solvent chemical potential. This will be reflected in a decrease in the pressure ($P - \Pi$) within the left compartment of the cell. It is essentially this difference in pressure between the two systems, which corresponds to the osmotic pressure of the solution, which is responsible for the difference between the chemical potentials $\mu_p(\phi_2,\phi_p\to0,T,\mu_1) - \mu_p(\phi_2\to0,\phi_p\to0,T,\mu_1)$ and $\mu_p(\phi_2,\phi_p\to0,T,P) - \mu_p(\phi_2\to0,\phi_p\to0,T,P)$.

A second and important difference between the present development and the earlier scaling-thermodynamic treatment is in the accounting of higher-order interactions. In particular, with reference to eq 1, a truncation was made in an expansion which produces an insignificant error only when $(N_2U_2/V)^2 \ll 1$. As was discussed in paper 1, near Θ-solvent conditions for the polymer and for very dilute polymer solutions, this constraint is readily satisfied.[19] However, at polymer concentrations, N_2/V, typically encountered in two-phase aqueous polymer systems, this condition is not (typically) satisfied.[19] Consequently, the incorporation of higher-order interactions was a significant advance in the evaluation of the standard-state protein chemical potential. It is interesting to note that errors introduced by the two approximations in paper 1, and discussed above, tend to cancel each other. That is, the correct evaluation of the protein chemical potential at constant T and P, as compared to that at constant T and μ_1, results in a lower protein chemical potential, while the incorporation of the higher-order interactions tends to increase the prediced protein chemical potential.

Finally, a few comments are in order to connect our conclusions with the suggestions of previous workers. First, our conclusions appear consistent with those of Forciniti and Hall,[57] who examined (using a virial expansion which was truncated at second order) the steric interactions between proteins and polymers (modeling both species for a variety of different geometries) and concluded that the influence of polymer molecular weight on the protein partition coefficient could not be accounted for by steric interactions alone. In addition, our conclusions regarding the presence of weak attractive interactions between the proteins studied and PEO are similar to those based on the lattice model results of Baskir et al.,[58,59] who also included an attractive interaction between the protein and the polymer. However, the mechanism through which the attraction influences the protein partitioning behavior is rather different in the two cases. Specifically, our approach recognizes the existence of identifiable polymer coils in the polymer solution phase and describes the interactions of *polymer coils* with the proteins. Baskir and co-workers considered the polymer solution phase to be a homogeneous polymer solution with a uniform concentration of polymer segments throughout the bulk polymer solution phase.[58,59] In contrast, in our description of protein partitioning, we have proposed that it is precisely this transition from the dilute to the entangled polymer solution regimes (with increasing PEO molecular weight) which is the underlying cause of the observed protein partitioning behavior accompanying a change in PEO molecular weight.

In concluding, we have presented a new formulation for the free energy of mixing solutions of proteins and identifiable polymer coils and have used it to describe experimental observations on the partitioning of proteins in two-phase aqueous PEO–dextran systems. The physical situation we have treated was based on our previous scaling-thermodynamic approach, which revealed that in two-phase aqueous polymer systems containing low-molecular-weight PEO, identifiable PEO coils in the PEO-rich solution phase interact with the protein molecules. In

the free-energy formulation presented in this paper, we have emphasized the importance of including the penetrable and deformable nature of the polymer in the description of the polymer–polymer and protein–polymer interactions. Within the framework of the thermodynamic formulation presented, we have concluded that (1) the deformability and penetrability of the polymer coils to the proteins are essential features of protein–polymer interactions, (2) purely steric interactions between hydrophilic proteins (considered here) and PEO coils cannot account for the observed influence of PEO molecular weight on the protein partitioning behavior, (3) the contributions of interactions between PEO coils, which are a function of PEO molecular weight, represent an important influence on the observed protein partitioning behavior observed to accompany a change in PEO molecular weight, (4) the presence of weak attractive interactions, of strength 0.01 to 0.1 kT, is consistent with the observed influence of PEO molecular weight on the protein partitioning behavior, (5) deviations of the protein shape from spherical symmetry can significantly influence the predicted protein partitioning behavior, and (6) the evaluation of the protein chemical potential at constant solvent chemical potential, rather than at constant pressure, can significantly influence the predicted protein partitioning behavior. While the above conclusions are based on a comparison of the predicted protein partitioning behavior (a thermodynamic property of the system) with that observed in the PEO–dextran two-phase aqueous system, in a subsequent paper of this series we present the interpretation of neutron-scattering measurements (which reflect the average correlations in the solution) in solutions containing PEO and proteins, which lead to essentially similar conclusions.[50]

Acknowledgment. Support for this work was provided by the National Science Foundation (NSF) through the Biotechnology Process Engineering Center at MIT under Grant CDR-88-03014 and a NSF Presidential Young Investigator (PYI) Award to D.B. and by the Whitaker Foundation. In addition, D.B. was supported through NSF Grant No. DMR-84-18718, administered by the Center for Materials Science and Engineering at MIT. D.B. is also grateful for the support by the Texaco–Mangelsdorf Career Development Professorship at MIT as well as to BASF, BP America, Exxon, Kodak, and Unilever for providing PYI matching funds. N.L.A. is grateful to the George Murray Scholarship Fund of the University of Adelaide, Australia, for financial support. The authors wish to thank Leo Lue for helpful discussions.

Appendix A

The derivation of eq 2 is best described with reference to Figure 12, which depicts an imaginary cell divided by a membrane (dashed line) which partitions a pure solvent compartment (left compartment) from a compartment which contains solvent and two types of solute macromolecular species (right compartment). In what follows, the solvent will be denoted as component 1, and the solute species as components 2 and 3. Later, components 2 and 3 will be identified as the polymer and protein, respectively. The volume fraction of component i in the right compartment is ϕ_i (i = 1, 2, 3). The system is maintained at constant temperature, T. Since the membrane is only permeable to the solvent, the pressure, P, in the right compartment is different from the pressure, P', in the left compartment. In view of the semipermeable nature of the membrane, the pressure difference across the membrane corresponds to the osmotic pressure, Π, of the macromolecular solution; that is

$$P' + \Pi(T,P,\phi_2,\phi_3) = P \tag{A1}$$

Note that to define the intensive state of a three-component single-phase system, the Gibbs phase rule requires that four intensive and independent state variables be specified (for example, T, P, ϕ_2, ϕ_3).[49]

Consider the system in Figure 12 constrained in such a way that in the right compartment the total pressure, P, is held constant. The Gibbs–Duhem equation for the right compartment is given by

$$N_1\,d\mu_1(T,P,\phi_2,\phi_3) + N_2\,d\mu_2(T,P,\phi_2,\phi_3) + N_3\,d\mu_3(T,P,\phi_2,\phi_3) = 0 \tag{A2}$$

where N_i and μ_i(i = 1, 2, 3) are the number of molecules and the chemical potential of component i, respectively.[49] In addition, under conditions of solvent diffusional equilibrium between the two compartments, changes in the solvent chemical potentials in each compartment must be equal; that is

$$d\mu_1(T,P,\phi_2,\phi_3) = d\mu_1'(T,P') \tag{A3}$$

Furthermore, since the left compartment contains pure solvent, it follows that, at constant temperature, changes in the pure solvent chemical potential can only result from changes in the pressure P', of the left compartment. That is

$$d\mu_1'(T,P') = \left[\frac{\partial\mu_1'(T,P')}{\partial P'}\right]_T dP' \tag{A4}$$

Finally, expressing the Gibbs free energy of the left compartment, at constant temperature, as

$$dG'(T,P',N_1')_T = V'\,dP' + \mu_1'\,dN_1' \tag{A5}$$

leads to the Maxwell relation

$$\left[\frac{\partial\mu_1'(T,P')}{\partial P'}\right]_{T,N_1'} = \left[\frac{\partial V'}{\partial N_1'}\right]_{T,P'} = V^\circ_1 \tag{A6}$$

where V°_1 is the molecular volume of the pure solvent in the left compartment.[49] In view of eqs A3, A4, and A6 it follows that

$$d\mu_1(T,P,\phi_2,\phi_3) = V_1^\circ\,dP' \tag{A7}$$

At constant P, eq A1 implies that $dP' = -d\Pi(T,P,\phi_2,\phi_3)$. Using this result in eq A7, and subsequently inserting the resulting expression for $d\mu_1$ in eq A2 yields

$$N_2\,d\mu_2(T,P,\phi_2,\phi_3) + N_3\,d\mu_3(T,P,\phi_2,\phi_3) = N_1V^\circ_1\,d\Pi(T,P,\phi_2,\phi_3) \tag{A8}$$

Differentiating eq A8 with respect to ϕ_2 at constant T, P, and ϕ_3 yields

$$N_2\left[\frac{\partial\mu_2}{\partial\phi_2}\right]_{T,P,\phi_3} + N_3\left[\frac{\partial\mu_3}{\partial\phi_2}\right]_{T,P,\phi_3} = N_1V^\circ_1\left[\frac{\partial\Pi}{\partial\phi_2}\right]_{T,P,\phi_3} \tag{A9}$$

In general, the osmotic pressure in the right compartment is a function of temperature, T, pressure P, and the volume fractions, ϕ_2 and ϕ_3. For the case of incompressible solutes and constant temperature, T, assumed in this derivation, the osmotic pressure on the right-hand side of eq A9 becomes a function of only ϕ_2 and ϕ_3. Therefore, since the osmotic pressure is independent of both the system pressure and the solvent chemical potential

$$\left[\frac{\partial\Pi(\phi_2,\phi_3)}{\partial\phi_2}\right]_{T,P,\phi_3} = \left[\frac{\partial\Pi(\phi_2,\phi_3)}{\partial\phi_2}\right]_{T,\mu_1,\phi_3} \tag{A10}$$

In view of eq A10 and utilizing volume fraction units ($\phi_i = N_i V^\circ_i / V$, where V°_i is the molecular volume of component i and V is the volume of the right compartment), eq A9 leads to the central result that

$$\frac{\phi_2}{V^\circ_2}\left[\frac{\partial \mu_2}{\partial \phi_2}\right]_{T,P,\phi_3} + \frac{\phi_3}{V^\circ_3}\left[\frac{\partial \mu_3}{\partial \phi_2}\right]_{T,P,\phi_3} = \phi_1\left[\frac{\partial \Pi}{\partial \phi_2}\right]_{T,\mu_1,\phi_3} \quad \text{(A11)}$$

The importance of eq A11 rests in the fact that it relates the chemical potentials of the macromolecules at constant pressure, P (the left-hand side of eq A11) to a thermodynamic property of the same system at constant solvent chemical potential, μ_1. An equivalent expression to eq A11 can be obtained by differentiating eq A8 with respect to ϕ_3, rather than ϕ_2, at constant ϕ_2, T, and P.

To evaluate the right-hand side of eq A11, it is useful to consider an alternative constraint imposed on the system shown in Figure 12 where now the pressure P' in the left compartment is held constant (along with the temperature). Under these conditions, in view of eq A4, the solvent chemical potential in the left compartment, $\mu_1'(T,P')$, is constant. In that case, eq A3 implies that

$$d\mu_1(T,P,\phi_2,\phi_2) = d\mu_1'(T,P') = 0 \quad \text{(A12)}$$

In addition, at constant P', eq A1 implies that the pressure change in the right compartment, dP, is equal to the osmotic pressure change, $d\Pi$; that is

$$dP = d\Pi(T,P,\phi_2,\phi_3) \quad \text{(A13)}$$

For the right compartment, under isothermal conditions and using eq A12, the Gibbs–Duhem equation takes the form[49]

$$N_2\, d\mu_2(T,P,\phi_2,\phi_3) + N_3\, d\mu_3(T,P,\phi_2,\phi_3) = V\, dP \quad \text{(A14)}$$

Substituting eq A13 in eq A14 and utilizing volume fraction units lead to the result

$$\frac{\phi_2}{V^\circ_2} d\mu_2(T,P,\phi_2,\phi_3) + \frac{\phi_3}{V^\circ_3} d\mu_3(T,P,\phi_2,\phi_3) = d\Pi(T,P,\phi_2,\phi_3) \quad \text{(A15)}$$

Differentiating eq A15 with respect to ϕ_2 at constant T, μ_1, and ϕ_3 yields

$$\frac{\phi_2}{V^\circ_2}\left[\frac{\partial \mu_2}{\partial \phi_2}\right]_{T,\mu_1,\phi_3} + \frac{\phi_3}{V^\circ_3}\left[\frac{\partial \mu_3}{\partial \phi_2}\right]_{T,\mu_1,\phi_3} = \left[\frac{\partial \Pi}{\partial \phi_2}\right]_{T,\mu_1,\phi_3} \quad \text{(A16)}$$

Multiplying eq A16 by ϕ_1 and substituting the resulting expression for $\phi_1(\partial\Pi/\partial\phi_2)_{T,\mu_1,\phi_3}$ in the right-hand side of eq A11 yield

$$\frac{\phi_2}{V^\circ_2}\left[\frac{\partial \mu_2}{\partial \phi_2}\right]_{T,P,\phi_3} + \frac{\phi_3}{V^\circ_3}\left[\frac{\partial \mu_3}{\partial \phi_2}\right]_{T,P,\phi_3} = \frac{\phi_1\phi_2}{V^\circ_2}\left[\frac{\partial \mu_2}{\partial \phi_2}\right]_{T,\mu_1,\phi_3} + \frac{\phi_1\phi_3}{V^\circ_3}\left[\frac{\partial \mu_3}{\partial \phi_2}\right]_{T,\mu_1,\phi_3} \quad \text{(A17)}$$

The equivalent expression to eq A17, which accounts for the variation of the chemical potentials with respect to the volume fraction of component 3, is given by

$$\frac{\phi_2}{V^\circ_2}\left[\frac{\partial \mu_2}{\partial \phi_3}\right]_{T,P,\phi_2} + \frac{\phi_3}{V^\circ_3}\left[\frac{\partial \mu_3}{\partial \phi_3}\right]_{T,P,\phi_2} = \frac{\phi_1\phi_2}{V^\circ_2}\left[\frac{\partial \mu_2}{\partial \phi_3}\right]_{T,\mu_1,\phi_2} + \frac{\phi_1\phi_3}{V^\circ_3}\left[\frac{\partial \mu_3}{\partial \phi_3}\right]_{T,\mu_1,\phi_2} \quad \text{(A18)}$$

With the knowledge of the chemical potentials μ_2 and μ_3 at constant solvent chemical potential, that is, the terms on the right-hand sides of eqs A17 and A18, these two equations provide coupled differential equations whose solution yields expressions for the chemical potentials, μ_2 and μ_3, as a function of compositions, ϕ_2 and ϕ_3, at constant pressure, P, and temperature, T.

To connect the formulation presented above to the protein partitioning problem, we identify component 2 with the polymer species and component 3 with the protein species. Accordingly, component 3 is renamed as component p. It is noteworthy that in the protein partitioning case, the solution of eqs A17 and A18 for the protein and polymer chemical potentials is simplified considerably by the fact that we are concerned with the limit of vanishing protein concentration, namely, $\phi_p \to 0$.[19] Therefore, we do not need to solve eq A18 since this equation describes the dependence of the protein and polymer chemical potentials on protein concentration. Furthermore, in eq A17, the polymer chemical potential, μ_2, become independent of protein concentration; that is, in the limit of vanishing protein concentration, the contribution of the protein to the osmotic pressure is negligible, as compared to the polymer contribution. Thus, in eq A17, the terms describing the polymer chemical potential are independent of the terms involving the protein, while the protein chemical potential *is* dependent on the polymer presence (since this determines the osmotic pressure of the solution). Therefore, eq A17 yields the two equations

$$\frac{1}{V^\circ_2}\left[\frac{\partial \mu_2}{\partial \phi_2}\right]_{T,P,\phi_p} = \frac{\phi_1}{V^\circ_2}\left[\frac{\partial \mu_2}{\partial \phi_2}\right]_{T,\mu_1,\phi_p} \quad \text{(A19)}$$

and

$$\frac{1}{V^\circ_p}\left[\frac{\partial \mu_p}{\partial \phi_2}\right]_{T,P,\phi_p} = \frac{\phi_1}{V^\circ_p}\left[\frac{\partial \mu_p}{\partial \phi_2}\right]_{T,\mu_1,\phi_p} \quad \text{(A20)}$$

Note that eq A19 can be derived by considering simply a two-component system containing polymer and water. The solution of eq A19 provides the polymer chemical potential at constant pressure. However, since our interest is in the influence of the polymer concentration on the protein chemical potential, we need to solve only eq A20. Equation A20 can be rewritten as

$$\frac{1}{1-\phi_2}\left[\frac{\partial \mu_p}{\partial \phi_2}\right]_{T,P,\phi_p} = \left[\frac{\partial \mu_p}{\partial \phi_2}\right]_{T,\mu_1,\phi_p} \quad \text{(A21)}$$

where the approximation, $\phi_1 = 1 - \phi_2 - \phi_p = 1 - \phi_2$, valid for vanishing protein concentrations, has been used. Equation A21 is a central result that is used in section 2 to evaluate changes in the protein chemical potential at constant pressure from changes in the protein chemical potential occurring at constant solvent chemical potential (see eq 2). Specifically, the usefulness of eq A21 results from the fact that the term on the right-hand side has been evaluated previously from an equation of state for the case of hard-sphere mixtures.[40]

References and Notes

(1) Tanford, C. *Physical Chemistry of Macromolecules*; Wiley: New York, 1961.
(2) Flory, P. J. *Principles of Polymer Chemistry*; Cornell University Press: Ithaca, NY, 1986.
(3) de Gennes, P.-G. *Scaling Concepts in Polymer Physics*; Cornell University Press: Ithaca, NY, 1988.
(4) Wilcoxon, J. P.; Martin, J. E.; Schaefer, D. W. *Phys. Rev. A* **1989**, *39*, 2675.
(5) Lin, M. Y.; Lindsay, H. M.; Weitz, D. A.; Ball, R. C.; Klein, R.; Meakin, P. *Nature* **1989**, *339*, 360.
(6) Israelachvili, J. N.; Mitchell, D. J.; Ninham, B. W. *J. Chem. Soc., Faraday Trans. 2*, **1976**, *72*, 1525.
(7) Puvvada, S.; Blankschtein, D. *J. Chem. Phys.* **1990**, *92*, 3710 and references cited therein.
(8) Chevalier, Y.; Zemb, T. *Rep. Prog. Phys.* **1990**, *53*, 279.

(9) Albertsson, P. A. *Partition of Cell Particles and Macromolecules*; Wiley: New York, 1986.
(10) Walter, H.; Brooks, D. E.; Fisher, D. *Partitioning in Aqueous Two-Phase Systems*; Academic Press: New York, 1985.
(11) Sutherland, I. A.; Fisher, D. *Separations Using Aqueous Two-Phase Systems*; Plenum: New York, 1989.
(12) Cotton, J. P.; Farnoux, B.; Jannink, G. *J. Chem. Phys.* **1972**, *57*, 290.
(13) Farnoux, B.; Daoud, M.; Deck, D.; Jannink, G.; Ober, R. *J. Phys. (Paris)* **1975**, *36*, L-35.
(14) Daoud, M.; Cotton, J. P.; Farnoux, B.; Jannink, G.; Sarma, G.; Benoit, H.; Duplessix, R.; Picot, C.; de Gennes, P.-G. *Macromolecules* **1975**, *8*, 804.
(15) Momii, T.; Numasawa, N.; Kuwamamoto, K.; Nose, T. *Macromolecules* **1991**, *24*, 3964.
(16) Dill, K. A.; Alonso, D. O. V. *Protein Structure and Protein Engingeering* **1988**, *39*, 51.
(17) Tanner, R. E.; Herpigny, B.; Chen, S.-H.; Rha, C. K. *J. Chem. Phys.* **1982**, *76*, 3866.
(18) Guo, X. H.; Zhao, N. M.; Chen, S.-H.; Teixeira, J. *Biopolymers* **1990**, *29*, 335.
(19) Abbott, N. L.; Blankschtein, D.; Hatton, T. A. *Macromolecules* **1991**, *24*, 4334.
(20) Baskir, J. N.; Hatton, T. A.; Suter, U. W. *Biotechnol. Bioeng.* **1989**, *34*, 541.
(21) Abbott, N. L.; Blankschtein, D.; Hatton, T. A. *Bioseparation* **1990**, *1*, 191.
(22) Hustedt, H.; Kroner, K. H.; Stach, W.; Kula, M.-R. *Biotechnol. Bioeng.* **1978**, *20*, 1989.
(23) Albertsson, P.-A.; Cajarville, A.; Brooks, D. E.; Tjerneld, F. *Biochim. Biophys. Acta* **1987** *926*, 87.
(24) Abbott, N. L.; Blankschtein, D.; Hatton, T. A. *Macromolecules*, in press.
(25) Vrij, A. *Pure Appl. Chem.* **1976**, *48*, 471.
(26) de Hek, H.; Vrij, A. *J. Colloid Interface Sci.* **1981**, *84*, 409.
(27) Vincent, B.; Luckham, P. F.; Waite, F. A. *J. Colloid Interface Sci.* **1979**, *73*, 508.
(28) Patel, P. D.; Russel, W. B. *J. Colloid Interface Sci.* **1989**, *131*, 192.
(29) Patel, P. D.; Russel, W. B. *J. Colloid Interface Sci.* **1989**, *131*, 201.
(30) Dey, D.; Hirtzel, C. S. *Colloid Polym. Sci.* **1991**, *269*, 28.
(31) McQuarrie, D. A. *Statistical Mechanics*; Harper & Row: New York, 1976.
(32) Carnahan, N. F.; Starling, K. E. *J. Chem. Phys.* **1969**, *51*, 635.
(33) Carnahan, N. F.; Starling, K. E. *J. Chem. Phys.* **1970**, *53*, 600.
(34) Flory, P. J.; Krigbaum, W. R. *J. Chem. Phys.* **1950**, *18*, 1086.
(35) Zimm, B. H.; Stockmayer, W. H.; Fixman, M. *J. Chem. Phys.* **1953**, *21*, 1716.
(36) Orofino, T. A.; Flory, P. J. *J. Chem. Phys.* **1957**, *26*, 1067.
(37) Wall, F. T.; Mandel, F. *J. Chem. Phys.* **1975**, *63*, 4592.
(38) Hermans, J. *J. Chem. Phys.* **1982**, *77*, 2193.
(39) Hermans, J. J.; Hermans, J. *J. Polym. Sci.* **1984**, *22*, 279.
(40) Jansen, J. W.; de Kruif, C. G.; Vrij, A. *J. Colloid Interface Sci.* **1986**, *114*, 471.
(41) Flory, P. J. *Statistical Mechanics of Chain Molecules*; Wiley: New York, 1968.
(42) Gobush, W.; Solc, K.; Stockmayer, W. H. *J. Chem. Phys.* **1974**, *60*, 12.
(43) des Cloizeaux, J.; Jannink, G. *Polymers in Solution: Their Modeling and Structure*; Clarendon Press: Oxford, 1990.
(44) Cabane, B.; Duplessix, R. *J. Phys. (Paris)* **1982**, *43*, 1529.
(45) Haynes, C. A.; Beynon, R. A.; King, R. S.; Blanch, H. W.; Prausnitz, J. *J. Chem. Phys.* **1989**, *93*, 5612.
(46) Edmond, E.; Ogston, A. G. *Biochem. J.* **1968**, *109*, 569.
(47) Rogers, J. A.; Tam, T. *Can. J. Pharm. Sci.* **1977**, *12*, 65.
(48) Cabane, B.; Duplessix, R. *J. Phys. (Paris)* **1987**, *48*, 651.
(49) Modell, M.; Reid, R. C. *Thermodynamics and Its Applications*; Prentice-Hall: Englewood Cliffs, NJ, **1983**.
(50) Abbott, N. L.; Blankschtein, D.; Hatton, T. A. *Macromolecules*, following paper in this issue.
(51) Jansons, K. M.; Phillips, C. G. *J. Colloid Interface Sci.* **1990**, *137*, 75.
(52) Creighton, T. E. *Proteins: Structures and Molecular Properties*; Freeman: New York, 1984.
(53) Peters. T. *Adv. Protein Chem.* **1985**, *37*, 161.
(54) Jansen, J. W.; de Kruif, C. G.; Vrij, A. *J. Colloid Interface Sci.* **1986**, *114*, 481.
(55) Jansen, J. W.; de Kruif, C. G.; Vrij, A. *J. Colloid Interface Sci.* **1986**, *114*, 492.
(56) Israelachvili, J. N. *Intermolecular and Surface Forces with Applications to Colloidal and Biological Systems*; Academic Press: London, 1985.
(57) Forciniti, D.; Hall, C. K. *ACS Symp. Ser.* **1990**, *419*, 53.
(58) Baskir, J. N.; Hatton, T. A.; Suter, U. W. *Macromolecules* **1987**, *20*, 1300.
(59) Baskir, J. N.; Hatton, T. A.; Suter, U. W. *J. Phys. Chem.* **1989**, *93*, 2111.
(60) Barker, J. A.; Henderson, D. *J. Chem. Phys.* **1967**, *47*, 2856.

Registry No. PEO, 25322-68-3; dextran, 9004-54-0.